

Daniela Ferrara, Andre Romano, and Jay S. Duker

---

## Contents

5.1	<b>Introduction</b> .....	79
5.2	<b>Optical Coherence Tomography as a Valuable Tool to Investigate the Choroid</b> .....	79
5.2.1	Fourier-Domain Optical Coherence Tomography Technologies .....	79
5.2.2	Structural Optical Coherence Tomography .....	80
5.2.3	Optical Coherence Tomography Angiography .....	81
5.3	<b>Normal Choroidal Thickness on Structural Optical Coherence Tomography</b> .....	83
5.4	<b>Normal Choroidal Morphology on Structural En Face Optical Coherence Tomography</b> .....	84
5.5	<b>Normal Choroidal Morphology on Optical Coherence Tomography Angiography</b> .....	85
	<b>References</b> .....	86

---

D. Ferrara, MD, PhD (✉)  
Tufts University School of Medicine,  
Boston, MA, USA  
e-mail: [daniela@ferrara.md](mailto:daniela@ferrara.md)

A. Romano, MD, PhD  
Department of Ophthalmology, Federal University  
Sao Paulo, Sao Paulo, Brazil

University of Miami, Miller School of Medicine,  
Miami, FL, USA

Neovista Eye Center, Americana, Brazil

J.S. Duker, MD  
Tuft Medical Center, Tufts University School of  
Medicine, Boston, MA, USA

---

## 5.1 Introduction

Recent technological advances in ophthalmic imaging, especially those in optical coherence tomography (OCT), revealed morphological changes of the choroid related to a wide number of pathological chorioretinal conditions, indicating a pivotal role in underlying disease mechanisms, in natural history of diseases, and also in response to therapeutic interventions.

OCT now permits the acquisition of high-speed, high-resolution imaging that generates tridimensional, depth-resolved optical reconstruction of the choroid. The ability to better characterize the in vivo morphology of the normal choroid is of fundamental importance to understand the role of the choriocapillaris and choroidal vasculature in physiological and pathological states of the eye.

---

## 5.2 Optical Coherence Tomography as a Valuable Tool to Investigate the Choroid

### 5.2.1 Fourier-Domain Optical Coherence Tomography Technologies

The physics of the OCT device plays a key role when investigating the choroid on OCT. Spectral-domain (SD)-OCT is the standard for diagnosis

and management of chorioretinal disorders in the clinical practice, but the documentation of the choroid may be compromised by limited depth of penetration (~850 nm), even when applying the enhanced depth imaging (EDI) method (Adhi et al. 2014; Spaide et al. 2008). The EDI-OCT is an acquisition technique that generally exhibits better quality of the choroid and choroidal-scleral interface, because the peak sensitivity is displaced posteriorly. By placing the zero-delay line toward the sclera, rather than at the level of the posterior vitreous, the roll-off sensitivity does not compromise the tomographic registration (Spaide et al. 2008; Spaide 2010). Although valuable to investigate the choroid in full thickness, this technique does not contribute significantly to documentation of the choriocapillaris given its proximity to the retinal pigment epithelium (RPE) (Spaide 2009).

Swept-source (SS)-OCT is a modified Fourier-domain and depth-resolved technology that offers potential advantages over SD-OCT, including reduced sensitivity roll-off with imaging depth, higher detection efficiencies, improved imaging range, adaptability to longer imaging wavelengths of ~1050 nm that improve penetration of the choroid, and higher image acquisition speeds (Unterhuber et al. 2005). SS-OCT employs a wavelength sweeping laser light source and a photodiode detector that records the interference of the backscattered light from the retina, while in SD-OCT a broadband light source is used, and a spectrometer and line scan camera record the interference (Potsaid et al. 2010). The improved performance of SS-OCT enables higher density raster scan protocols and deeper image penetration, contributing to better visualization of the choriocapillaris and choroidal vessels (Adhi et al. 2015; Ferrara et al. 2014; Montaghianezam et al. 2012; Sohrab et al. 2012; Srinivasan et al. 2008).

Despite potential advantages of SS-OCT in comparison to SD-OCT to investigate the choroid, the differences between the two technologies are related to the qualitative assessment. Quantitative observations seem to be significantly correlated and highly reproducible, assuming that retinochoroidal and choroidal-scleral interfaces are clearly visible (Branchini et al.

2012; Copete et al. 2014; Ellabban et al. 2012; Hirata et al. 2011; Matsuo et al. 2013; Tan et al. 2015; Yamashita et al. 2012).

## 5.2.2 Structural Optical Coherence Tomography

Cross-sectional OCT imaging is widely used in the clinical ophthalmological practice and has been considered a fundamental tool in the diagnosis and management of chorioretinal diseases. The integrity of the RPE/Bruch's membrane/choriocapillaris complex and the subfoveal total choroidal thickness are among the features of fundamental importance for clinical interpretation. Cross-sectional OCT, however, has limited ability to document in details the choriocapillaris and individual choroidal layers, even in normal eyes with preserved anatomy. Some studies have assessed in conjunction the choriocapillaris and medium-size choroidal vessels when using cross-sectional OCT (Adhi et al. 2013; Branchini et al. 2013).

En face OCT imaging is generated by successive alignment of multiple adjacent B-scans rendering a tridimensional dataset. It allows high-definition depth-resolved reconstruction of the choroidal tissue in a plane parallel to the anatomic structures, rather than in a perpendicular plane. En face OCT documents details of the choroid not readily appreciated on cross-sectional OCT, besides offering ideal correlation with other imaging modalities. Nonetheless, for optimal interpretation, both cross-sectional and en face OCT images should be analyzed in conjunction, in a multidimensional assessment. Although the identification of feeder arterioles and draining venules is limited even on en face OCT, choriocapillaris and medium-size and large-size choroidal vessels can be clearly identified (Adhi et al. 2015; Ferrara et al. 2014; Montaghianezam et al. 2012; Sohrab et al. 2012; Srinivasan et al. 2008). For such, post-acquisition image processing and registration is of fundamental importance. OCT image quality can be improved to correct eye movements, tilting, illumination, and image noise, for example. Another major aspect

to properly evaluate the choroid on en face OCT is image registration using the RPE or Bruch's membrane as a reference surface. This digital processing compensates the natural curvature of the back of the eye and, in result, permits documentation of each individual choroidal layer in one distinct plan (Figs. 5.1, 5.2, and 5.3).

### 5.2.3 Optical Coherence Tomography Angiography

OCT angiography is a recently developed technology that allows noninvasive documentation of vascular structures and is a useful investigative tool of the choriocapillaris and choroidal microvasculature in physiological

and pathological conditions. The basic principle of OCT angiography assumes that all other elements remaining static, the only difference between sequential OCT scans in a given location of the tissue is caused by the motion of erythrocytes within the vessels. It can be obtained with several different technologies, classified into two major groups: amplitude based and phase based. Important examples of amplitude-based technologies are the split-spectrum amplitude-decorrelation angiography (SSADA), scattering OCT, and speckle variance (Jia et al. 2012), while examples of phase-based technologies are phase-variance OCT and Doppler OCT (Fingler et al. 2007; Kim et al. 2011). All of these can be implemented in high-speed Fourier-domain OCT, either SD-OCT or SS-OCT systems.

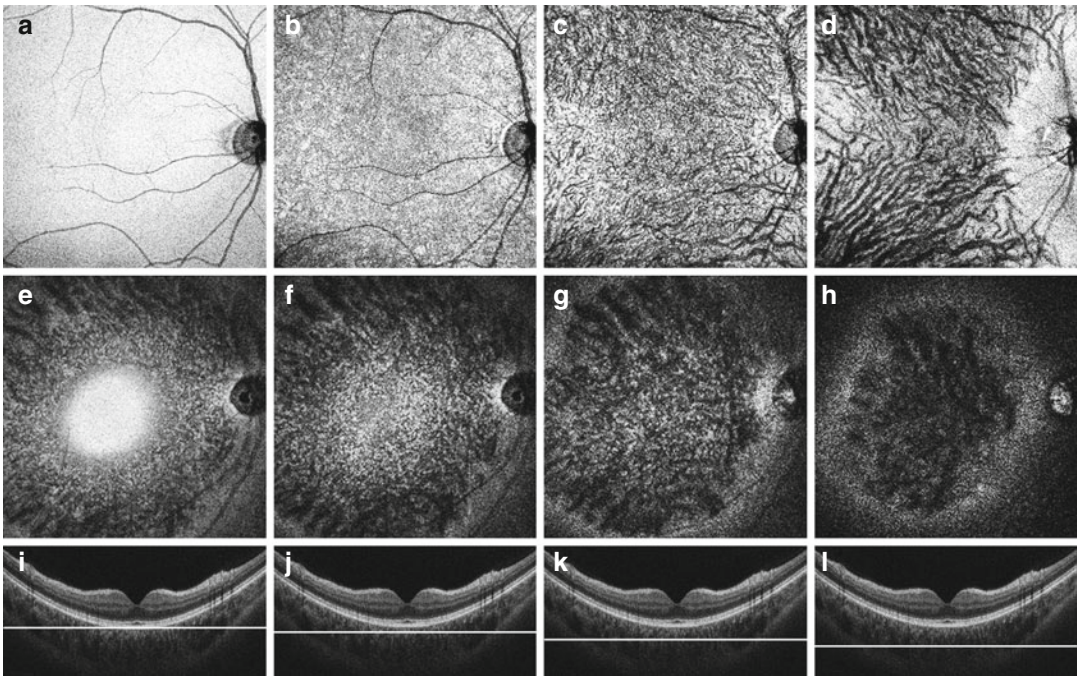


**Fig. 5.1** Structural en face optical coherence tomography (OCT) of normal eyes obtained with swept-source OCT. In the *upper row*, en face OCT was registered taking the Bruch's membrane as a reference surface to compensate the natural curvature of the eye. Each scan documents an individual choroidal layer, as follows: retinal pigment epithelium (RPE) (a), choriocapillaris (b), inner choroid (c), and outer choroid (d). Note at the level of the outer choroid (d) a peripapillary area without choroidal vessels, correspondent to the so-called watershed zone. In the

*middle row*, original en face OCT scans without registration. Each scan documents multiple choroidal layers; the following levels are documented in the center of the scans: RPE (e), choriocapillaris (f), inner choroid (g), and outer choroid (h). In the *lower row*, cross-sectional OCT centered at the fovea. Individual choroidal layers are not readily appreciated. The horizontal lines indicate the level of en face scans, as follows: RPE (i), choriocapillaris (j), inner choroid (k), and outer choroid (l)

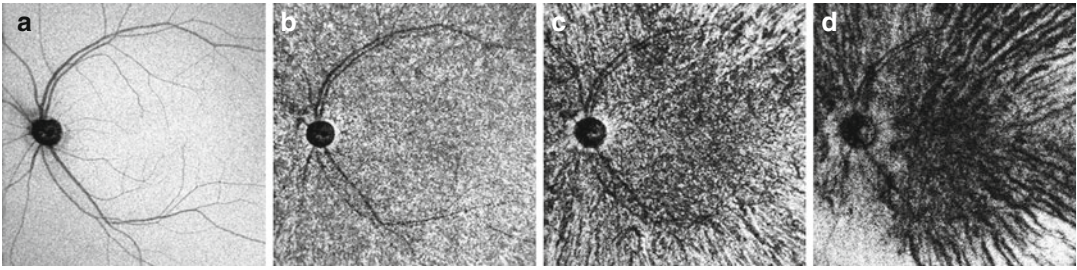


**Fig. 5.2** Structural en face optical coherence tomography (OCT) of normal eye obtained with swept-source OCT. Images were registered taking the Bruch's membrane as a reference surface to compensate the natural curvature of the eye. En face OCT at the level of the retinal pigment epithelium (a) is characterized by homogeneous hyperreflective layer. The only hyporeflexive structures are the optic disc and the shadowing artifact of overlying retinal vessels. En face OCT at the level of the choriocapillaris (b) shows homogeneous reticular pattern

throughout the scan. En face OCT at the level of the inner choroid (c) shows in the macular area a complex, interwoven network of short and relatively thin vascular segments crossing over each other and homogeneously distributed, while in extramacular areas the vessels are fewer in number. En face OCT scans at the level of the outer choroid (d) show wider vessels, interwoven in the center of the macula but assuming a distinct radial distribution beyond the macular area toward the equator

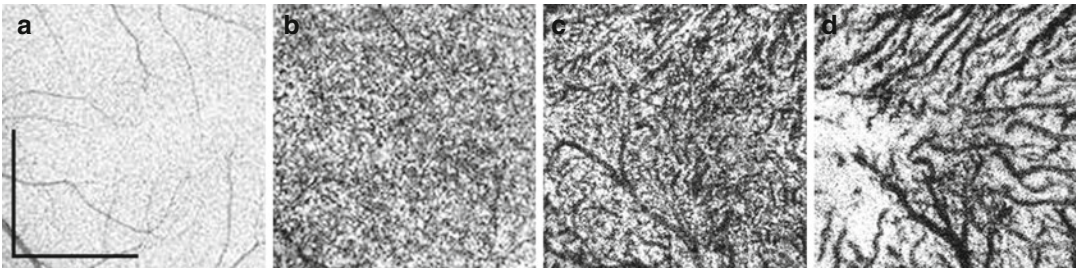


**Fig. 5.3** Structural en face optical coherence tomography (OCT) of normal eye obtained with a swept-source OCT prototype operating at 1050 nm. Images were registered taking the Bruch's membrane as a reference surface to compensate the natural curvature of the eye. Magnified

fields show details of the individual layers as follows: retinal pigment epithelium (a), choriocapillaris (b), inner choroid (c), and outer choroid (d). Vertical and horizontal scale bars measuring 1.5 mm

OCT angiography has fundamental differences when compared to standard fluorescein angiography or indocyanine green angiography; direct comparison between these methods is not always feasible and should be taken with caution. The proper interpretation of OCT angiography must consider the physical principles of imaging acquisition: images do not change throughout the acquisition process, and since no exogenous dye is used, leakage, staining, or pooling is not documented. On the other hand, it is subject to specific artifacts mostly related to the optical reconstruction of vascular tissues. One important limitation is the fact that OCT angiography

identifies the vascular flow within a limited dynamic range. There is a sensitivity limit, which is the slowest detectable flow determined by the elapsed time between sequential scans. There is also a saturation limit, which is the fastest detectable flow that is differentiated by the decorrelation signal. All these considerations are relevant when interpreting OCT angiography of the choroidal vasculature. Although the choroid has the highest blood flow per unit weight tissue in the human body (Alm and Bill 1973), the blood flow in the choriocapillaris and choroidal vasculature may occasionally be too slow or too fast to be documented by this imaging method.

### 5.3 Normal Choroidal Thickness on Structural Optical Coherence Tomography

While choroidal thinning on OCT has been associated with various pathological conditions such as AMD, age-related choroidal atrophy, and high myopia, it is important to note that the total choroidal thickness also varies widely in the normal population at both the subfoveal and the extramacular locations (Branchini et al. 2013; Flores-Moreno et al. 2013; Kim et al. 2011; Spaide 2009; Wei et al. 2013). Variability related with gender, age, axial length, and refractive error has been reported (Barteselli et al. 2012; Margolis and Spaide 2009; Sanchez-Cano et al. 2014). It may be challenging, therefore, to establish normative values or to identify a clear threshold between normal and pathological choroidal thickness in the clinical setting.

The subfoveal total choroidal thickness has been found to correlate significantly with age, and progressive subfoveal total choroidal thinning occurs in normal aging eyes (Fujiwara et al. 2009; Ikuno and Tano 2009; Ikuno et al. 2010; Manjunath et al. 2010; Margolis and Spaide 2009; Hirata et al. 2011; Ooto et al. 2015). Subfoveal choroidal thickness was also found to be negatively correlated with axial length (Benavente-Perez et al. 2010; Esmaelpour et al. 2010; Hirata et al. 2011; Li et al. 2011; Ooto et al. 2015) and positively correlated with refractive error (Fujiwara et al. 2009; Ikuno and Tano 2009; Ikuno et al. 2010). Diurnal variations on the same individuals were also reported (Brown et al. 2009; Ikuno et al. 2010; Tan et al. 2012) and seem to correlate with diurnal variations of the ocular axial length (Chakraborty et al. 2011).

Progressive choroidal thinning in normal aging eyes was documented in both *post-mortem* histopathological studies and in vivo investigations, using either cross-sectional OCT or en face OCT (Adhi et al. 2015; Ferrara et al. 2016; Ikuno et al. 2010; Manjunath et al. 2011; Margolis and Spaide 2009; McLeod and Luttly 1994; Spaide 2009; Wei et al. 2013). Investigations on en face OCT suggested that the proportion between individual choroidal layers may also change in older individuals,

and it is possible that in normal aging eyes, the choriocapillaris loss may be relatively more significant than loss of medium-size and large-size choroidal vessels. Morphological changes in the choriocapillaris and choroidal vasculature patterns have not been correlated so far with the normal aging process (Ferrara et al. 2016).

Caution is needed when comparing choroidal thickness measurements reported in different studies available in the literature, because variations in demographic or clinical characteristics may preclude a direct correlation between different cohorts. In one of the first attempts to obtain normative values for the normal population using SD-OCT, the mean subfoveal total choroidal thickness in a small group of patients, mean age of 50 years, was found to be 287  $\mu\text{m}$ , which was found to decrease approximately 15  $\mu\text{m}$  for each decade of life (Margolis and Spaide 2009). Subfoveal total choroidal thickness seems to decrease especially after the age of 40 (Ferrara et al. 2016; Ruiz-Medrano et al. 2014). In another cohort, the following measurements were found on SS-OCT for each age range: 325.6 $\pm$ 51.1  $\mu\text{m}$  (0–10 years), 316.7 $\pm$ 90.1  $\mu\text{m}$  (11–20 years), 313.9 $\pm$ 80.3  $\mu\text{m}$  (21–40 years), 264.6 $\pm$ 79.3  $\mu\text{m}$  (41–60 years), and 276.3 $\pm$ 88.8  $\mu\text{m}$  (older than 60 years), in addition to different choroidal thickness profiles for each age group with greater variations in the temporal quadrant of the fundus (Ruiz-Medrano et al. 2014). Several other studies have reported highly variable values for mean subfoveal total choroidal thickness, investigating cohorts of different demographic characteristics (Benavente-Perez et al. 2010; Hirata et al. 2011). As a gross estimate, in vivo subfoveal total choroidal thinning was considered to progress 1.56  $\mu\text{m}$  per year, which is higher than 1.1  $\mu\text{m}$  per year estimated from *post-mortem* specimens (Margolis and Spaide 2009). Although several aspects can justify such difference, to some extent it may be related to the lack of blood flow in histological examination (Feeney-Burns et al. 1990; Ramrattan et al. 1994; Sarks 1976).

In addition, normal variations of the choroidalscleral contour also contribute to the variability in total choroidal thickness measurements, which vary throughout the fundus (Adhi et al. 2014;

Branchini et al. 2013). In normal eyes the choroid is thickest under the fovea, showing marked thinning toward the periphery in all four quadrants – nasal, temporal, superior, and inferior (Esmaeelpour et al. 2010; Hirata et al. 2011; Ikuno et al. 2010; Manjunath et al. 2010). The peripapillary total choroidal thickness was found to be the thinnest inferiorly to the optic disk (Ho et al. 2011; Tanabe et al. 2012).

The suprachoroidal layer is not commonly observed on OCT in normal eyes. It is estimated to be documented on cross-sectional OCT in only 5% of healthy emmetropic eyes as two distinct bands: an upper hyperreflective band corresponding to the suprachoroidal layer and a lower hyporefective band supposedly corresponding to the suprachoroidal space, which in vivo was previously visualized only in eyes with choroidal effusion (Michalewska et al. 2015).

---

#### 5.4 Normal Choroidal Morphology on Structural En Face Optical Coherence Tomography

The normal choroid has been investigated on recent research using depth-resolved en face OCT, extracted from tridimensional datasets, which is strikingly superior than cross-sectional OCT for this matter. Most of these recent studies use SS-OCT, since it documents deeper structures better than SD-OCT (Adhi et al. 2015; Ferrara et al. 2014; Ferrara et al. 2016; Montaghianezam et al. 2012; Sohrab et al. 2012; Sohrab and Fawzi 2013; Srinivasan et al. 2008). The morphological features of the choroid do not seem to present qualitative changes during normal aging, although quantitative changes are typically observed, as discussed above (Ferrara et al. 2016).

Structural en face OCT of the RPE in normal eyes is regularly homogeneous and hyperreflective throughout the scan, including the macular and peripapillary areas. The only hyporefective elements correspond to the optic disk and to the tomographic shadowing artifact of the overlying normal retinal vessels (Ferrara et al. 2016). These references are important for the proper

interpretation of the image, because this artifact is transmitted on en face layers throughout the volumetric dataset and should not be confounded with actual choroidal vessels.

Structural en face OCT of the choriocapillaris and choroidal microvasculature are challenging to be obtained, even in normal eyes, because of the small caliber and complexity of the vascular network. No distinct capillary vessels can be readily identified on en face OCT, with the current available technology. Instead, they appear as homogeneous reticular pattern throughout the scan, including the macular and peripapillary areas, lying at a level external to the RPE and internal to the choroidal vasculature. Microvascular choroidal anastomoses between the choriocapillaris and terminal arterioles or venules from the inner choroid are also present at this level. However, since both choriocapillaris and microvascular anastomosis appear on en face OCT as a reticular pattern, no tomographic distinction can be made between them (Ferrara et al. 2016) (Fig. 5.4).

Structural en face OCT of the inner and outer choroid in normal eyes has distinct characteristics, depending on the area of the fundus and on the level of the scan. In the macular area, choroidal vessels appear on en face OCT as highly complicated, interwoven, short vascular segments crossing over each other. In en face scans of extramacular areas, choroidal vessels are straighter and fewer in number representing a radial distribution outward from the center of the macula toward the equator (Ferrara et al. 2016). En face scans at the level of the inner choroid present thinner vessels, homogeneously distributed in the macular area through the topography of the retinal vascular arcades. En face scans at the level of the outer choroid present wider vessels, interwoven in the center of the macula but assuming clear radial distribution beyond the macular area toward the equator (Montaghianezam et al. 2012; Sohrab et al. 2012). No distinct anatomic boundary can be determined between inner and outer choroid, since vessel caliber and distribution change in a progressive gradient. Also, arteries and veins cannot be differentiated based on tomographic features (Ferrara et al. 2016).

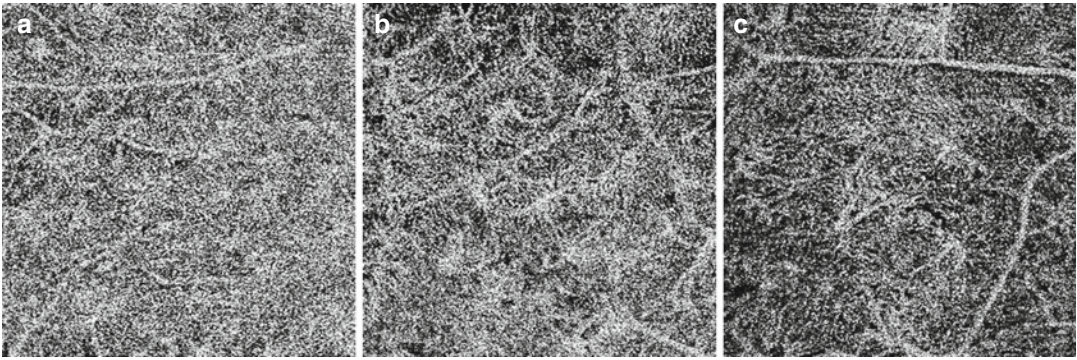


**Fig. 5.4** Optical coherence tomography (OCT) angiography of a normal eye obtained with ultrahigh speed swept-source OCT prototype operating at 1060 nm (Choi et al. 2013). Scans document the choriocapillaris in different

sectors of the fundus. In the center of the macula (a), the choriocapillaris shows dense reticular appearance, while it shows less dense appearance in the mid-periphery (b) and a lobular appearance toward the equator (c)

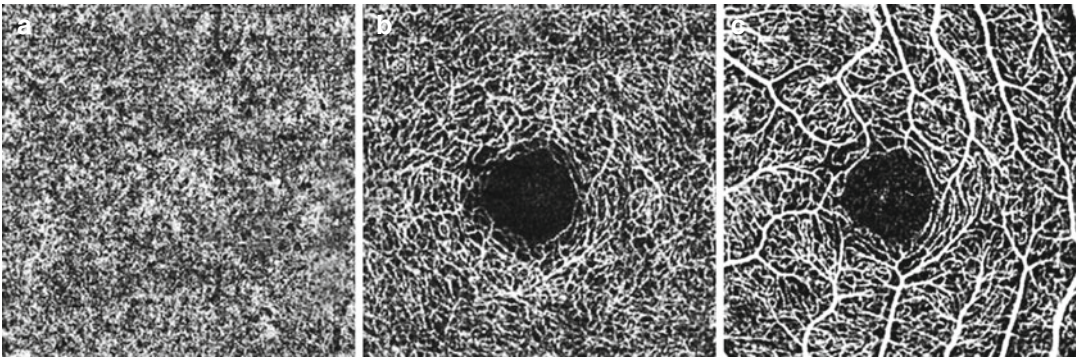


**Fig. 5.5** Optical coherence tomography (OCT) angiography of a normal eye obtained with a commercially available spectral-domain OCT. OCT angiography documents the choriocapillaris (a) in the center of the macular area.

OCT angiography of the retinal circulation is also shown in comparison with the choroidal circulation, at the level of the deep retinal plexus (b) and superficial retinal plexus (c)

A peripapillary area of preserved choriocapillaris but absent medium-size and large-size choroidal vessels, corresponding to the angiographic description of the so-called watershed zone (Hayreh 1975; Hayreh 1990), can be documented on en face OCT (Fig. 5.5).

## 5.5 Normal Choroidal Morphology on Optical Coherence Tomography Angiography

OCT angiograms can be generated by tridimensional rendering from cross-sectional images of the speckle decorrelation between sequential

scans, repeatedly acquired on the same position, as discussed above. Assuming the documented tissue remains static, all scans will be identical, except where there is erythrocyte motion within the blood vessels. This motion results in local oscillation of backscattered light intensity, which can be calculated by comparing each pixel on the scans and results in a motion contrast. A volumetric dataset documenting the tissue on OCT angiography can be obtained by performing this operation for all transverse positions of the scan (Choi et al. 2013).

As a general rule discussed above, it is important to take into account artifacts for proper interpretation of the OCT images. Therefore, the choroidal vasculature should not be confounded

with the shadowing artifact from large retinal blood vessels, which have lower signal levels and more rapidly fluctuating speckle pattern to occur below them (Choi et al. 2013).

OCT angiogram of the choriocapillaris documents distinct capillary density and pattern depending on the location in the fundus, in agreement with previous characterization on histopathological studies (McLeod and Luty 1994; Olver 1990; Yoneya 1987; Zhang 1994). In the center of the macula, the choriocapillaris exhibits dense reticular or honeycomb appearance, while it has less dense and lobular structure toward the equator. OCT angiography may be a better tool to differentiate choriocapillaris from feeding arterioles and draining vessels, in comparison to structural en face OCT, because the speckle decorrelation is related to the erythrocyte speed. Nonetheless, the differentiation between arterioles and venules on OCT angiography has been attempted but is still challenging (Choi et al. 2013). The same agreement between in vivo and post-mortem spatial characterization of the choroidal vessels was observed on OCT angiography of the inner choroid (Choi et al. 2013). Larger choroidal vessels have higher flow rates and therefore can only be visualized with en face OCT intensity images, which generates contrast from light scattering and fringe washout effects instead of speckle decorrelation.

## References

- Adhi M, Brewer E, Waheed NA, Duker JS (2013) Analysis of morphological features and vascular layers of choroid in diabetic retinopathy using spectral-domain optical coherence tomography. *JAMA Ophthalmol* 131:1267–1274
- Adhi M, Liu JJ, Qavi AH, Grulkowski I, Lu CD, Mohler KJ, Ferrara D, Kraus MF, Baumal CR, Witkin AJ, Waheed NK, Hornegger J, Fujimoto JG, Duker JS (2014) Choroidal analysis in healthy eyes using swept source optical coherence tomography compared with spectral domain optical coherence tomography. *Am J Ophthalmol* 157:1272–1281
- Adhi M, Ferrara D, Mullins RF, Baumal CR, Mohler KJ, Kraus MF, Liu J, Badaro E, Alasil T, Hornegger J, Fujimoto JG, Duker JS, Waheed NK (2015) Characterization of choroidal layer in normal aging eyes using enface swept-source optical coherence tomography. *PLoS One* 10:e0133080
- Alm A, Bill A (1973) Ocular and optic nerve blood flow at normal and increased intraocular pressures in monkeys (*Macaca irus*): a study with radioactively labelled microspheres including flow determinations in brain and some other tissues. *Exp Eye Res* 15:15–19
- Barteselli G, Chhablani J, El-Emam S, Wang H, Chuang J, Kosak I, Cheng L, Bartsch DU, Freeman WR (2012) Choroidal volume variations with age, axial length, and sex in healthy subjects: a three-dimensional analysis. *Ophthalmology* 119:2572–2578
- Benavente-Perez A, Hosking SL, Logan NS, Bansal D (2010) Reproducibility-repeatability of choroidal thickness calculation using optical coherence tomography. *Optom Vis Sci* 87:867–872
- Branchini L, Regatieri CV, Flores-Moreno I, Baumann B, Fujimoto JG, Duker JS (2012) Reproducibility of choroidal thickness measurements across three spectral domain optical coherence tomography systems. *Ophthalmology* 119:119–123
- Branchini LA, Adhi M, Regatieri CV, Nandakumar N, Liu JJ, Laver N, Fujimoto JG, Duker JS (2013) Analysis of choroidal morphologic features and vasculature in healthy eyes using spectral-domain optical coherence tomography. *Ophthalmology* 120:1901–1908
- Brown JS, Flitcroft DI, Ying GS, Francis EL, Schmid GF, Quinn GE, Stone RA (2009) In vivo human choroidal thickness measurements: evidence for diurnal fluctuations. *Invest Ophthalmol Vis Sci* 50:5–12
- Chakraborty R, Read SA, Collins MJ (2011) Diurnal variations in axial length, choroidal thickness, intraocular pressure, and ocular biometrics. *Invest Ophthalmol Vis Sci* 52:5121–5134
- Choi W, Mohler K, Potsaid B, Lu CD, Liu JJ, Jayaraman V, Cable AE, Duker JS, Huber R, Fujimoto JG (2013) Choriocapillaris and choroidal microvasculature imaging with ultrahigh speed OCT angiography. *PLoS One* 8:e81499
- Copete S, Flores-Moreno I, Montero JA, Duker JS, Ruiz-Moreno JM (2014) Direct comparison of spectral-domain and swept-source OCT in the measurement of choroidal thickness in normal eyes. *Br J Ophthalmol* 98:334–338
- Ellabban AA, Tsujikawa A, Matsumoto A, Oginio K, Hangai M, Ooto S, Yamashiro K, Akiba M, Yoshimura N (2012) Macular choroidal thickness and volume in eyes with angioid streaks measured by swept source optical coherence tomography. *Am J Ophthalmol* 153:1133–1143
- Esmaeelpour M, Povazay B, Hermann B, Hofer B, Kajic V, Kapoor K, Sheen NJ, North RV, Drexler W (2010) Three-dimensional 1060-nm OCT: choroidal thickness maps in normal subjects and improved posterior segment visualization in cataract patients. *Invest Ophthalmol Vis Sci* 51:5260–5266
- Feeney-Burns L, Burns RP, Gao CL (1990) Age-related macular changes in humans over 90 years old. *Am J Ophthalmol* 109:265–278



- Ferrara D, Mohler KJ, Waheed N, Adhi M, Liu JJ, Grulkowski I, Kraus MF, Baurnal C, Hornegger J, Fujimoto JG, Duker JS (2014) En face enhanced-depth swept-source optical coherence tomography features of chronic central serous chorioretinopathy. *Ophthalmology* 121:719–726
- Ferrara D, Waheed NK, Duker JS (2016) Investigating the choriocapillaris and choroidal vasculature with new optical coherence tomography technologies. *Prog Retin Eye Res* 52:130–155
- Fingler J, Schwartz D, Yang C, Fraser SE (2007) Mobility and transverse flow visualization using phase variance contrast with spectral domain optical coherence tomography. *Opt Express* 15:12636–12653
- Flores-Moreno I, Lugo F, Duker JS, Ruiz-Moreno JM (2013) The relationship between axial length and choroidal thickness in eyes with high myopia. *Am J Ophthalmol* 155:314–319
- Fujiwara T, Imamura Y, Margolis R, Slakter JS, Spaide RF (2009) Enhanced depth imaging optical coherence tomography of the choroid in highly myopic eyes. *Am J Ophthalmol* 148:445–450
- Hayreh SS (1975) Segmental nature of the choroidal vasculature. *Br J Ophthalmol* 59:631–648
- Hayreh SS (1990) In vivo choroidal circulation and its watershed zones. *Eye (Lond)* 4:273–289
- Hirata M, Tsujikawa A, Matsumoto A, Hangai M, Ooto S, Yamashiro K, Akiba M, Yoshimura N (2011) Macular choroidal thickness and volume in normal eyes measured by swept-source optical coherence tomography. *Invest Ophthalmol Vis Sci* 52:4971–4978
- Ho J, Branchini L, Regatieri C, Krishnan C, Fujimoto JG, Duker JS (2011) Analysis of normal peripapillary choroidal thickness via spectral domain optical coherence tomography. *Ophthalmology* 118:2001–2007
- Ikuno Y, Kawaguchi K, Nouchi T, Yasuno Y (2010) Choroidal thickness in healthy Japanese subjects. *Invest Ophthalmol Vis Sci* 51:2173–2176
- Ikuno Y, Tano Y (2009) Retinal and choroidal biometry in highly myopic eyes with spectral-domain optical coherence tomography. *Invest Ophthalmol Vis Sci* 50:3876–3880
- Jia Y, Tan O, Tokayer J, Potsaid B, Wang Y, Liu JJ, Kraus MF, Subhash H, Fujimoto JG, Hornegger J, Huang D (2012) Split-spectrum amplitude-decorrelation angiography with optical coherence tomography. *Opt Express* 20:4710–4725
- Kim SW, Oh J, Kwon SS, Yoo J, Huh K (2011) Comparison of choroidal thickness among patients with healthy eyes, early age-related maculopathy, neovascular age-related macular degeneration, central serous chorioretinopathy, and polypoidal choroidal vasculopathy. *Retina* 31:1904–1911
- Li XQ, Larsen M, Munch IC (2011) Subfoveal choroidal thickness in relation to sex and axial length in 93 Danish university students. *Invest Ophthalmol Vis Sci* 52:8438–8441
- Manjunath V, Taha M, Fujimoto JG, Duker JS (2010) Choroidal thickness in normal eyes measured using Cirrus HD optical coherence tomography. *Am J Ophthalmol* 150:325–329
- Manjunath V, Goren J, Fujimoto JG, Duker JS (2011) Analysis of choroidal thickness in age-related macular degeneration using spectral-domain optical coherence tomography. *Am J Ophthalmol* 152:663–668
- Margolis R, Spaide RF (2009) A pilot study of enhanced depth imaging optical coherence tomography of the choroid in normal eyes. *Am J Ophthalmol* 147:811–815
- Matsuo Y, Sakamoto T, Yamashita T, Tomita M, Shirasawa M, Terasaki H (2013) Comparisons of choroidal thickness of normal eyes obtained by two different spectral-domain OCT instruments and one swept-source OCT instrument. *Invest Ophthalmol Vis Sci* 54:7630–7636
- McLeod DS, Luty GA (1994) High-resolution histologic analysis of the human choroidal vasculature. *Invest Ophthalmol Vis Sci* 35:3799–3811
- Michalewska Z, Michalewski J, Nawrocka Z, Dulczewska-Cichecka K, Nawrocki J (2015) Suprachoroidal layer and suprachoroidal space delineating the outer margin of the choroid in swept-source optical coherence tomography. *Retina* 35:244–249
- Montaghianezam R, Schwartz DM, Fraser SE (2012) In vivo human choroidal vascular pattern visualization using high-speed swept-source optical coherence tomography at 1060 nm. *Invest Ophthalmol Vis Sci* 53:2337–2348
- Mullins RF, Johnson MN, Faidley EA, Skeie JM, Huang J (2011) Choriocapillaris vascular dropout related to density of drusen in human eyes with early age-related macular degeneration. *Invest Ophthalmol Vis Sci* 52:1606–1612
- Olver JM (1990) Functional anatomy of the choroidal circulation: methyl methacrylate casting of human choroid. *Eye* 4:262–272
- Ooto S, Hangai M, Yoshimura N (2015) Effects of sex and age on the normal retinal and choroidal structures on optical coherence tomography. *Curr Eye Res* 40:213–225
- Potsaid B, Baumann B, Huang D, Barry S, Cable AE, Schuman JS, Duker JS, Fujimoto JG (2010) Ultrahigh speed 1050 nm swept source/fourier domain OCT retinal and anterior segment imaging at 100,000 to 400,000 axial scans per second. *Opt Express* 18:20029–20048
- Ramrattan RS, van der Schaft TL, Mooy CM, de Bruijn WC, Mulder PG, de Jong PT (1994) Morphometric analysis of Bruch membrane, the choriocapillaris, and the choroid in aging. *Invest Ophthalmol Vis Sci* 35:2857–2864
- Ruiz-Medrano J, Flores-Moreno I, Pena-Garcia P, Montero JA, Duker JS, Ruiz-Moreno JM (2014) Macular choroidal thickness profile in a healthy population measured by swept-source optical coherence tomography. *Invest Ophthalmol Vis Sci* 55:3532–3542
- Sanchez-Cano A, Orduna E, Segura F, Lopez C, Cuenca N, Abecia E, Pinilla I (2014) Choroidal thickness and

- volume in healthy young white adults and the relationships between them and axial length, ametropia and sex. *Am J Ophthalmol* 158:574–583
- Sarks SH (1976) Ageing and degeneration in the macular region: a clinic-pathological study. *Br J Ophthalmol* 60:324–341
- Sohrab MA, Fawzi AA (2013) Review of en-face choroidal imaging using spectral-domain optical coherence tomography. *Med Hypothesis Discov Innov Ophthalmol* 2:69–73
- Sohrab M, Wu K, Fawzi AA (2012) A pilot study of morphometric analysis of choroidal vasculature in vivo, using en face optical coherence tomography. *PLoS One* 7:e48631
- Spaide RF (2009) Age related choroidal atrophy. *Am J Ophthalmol* 147:801–810
- Spaide RF (2010) Choroidal imaging with optical coherence tomography. In: Holz FG, Spaide RF (eds) *Medical retina focus on retinal imaging*. Springer, Berlin, pp 169–190
- Spaide RF, Koizumi H, Pozzoni MC (2008) Enhanced depth imaging spectral-domain optical coherence tomography. *Am J Ophthalmol* 146:496–500
- Srinivasan VJ, Adler DC, Chen Y, Gorczynska I, Huber R, Duker JS, Schuman JS, Fujimoto JG (2008) Ultrahigh-speed optical coherence tomography for three-dimensional and en face imaging of the retina and optic nerve head. *Invest Ophthalmol Vis Sci* 49:5103–5110
- Tan CS, Ngo WK, Cheong KX (2015) Comparison of choroidal thickness using swept-source and spectral domain optical coherence tomography in diseased and normal eyes. *Br J Ophthalmol* 99:354–358
- Tan CS, Ouyang Y, Ruiz H, Sadda SR (2012) Diurnal variation of choroidal thickness in normal, healthy subjects measured by spectral domain optical coherence tomography. *Invest Ophthalmol Vis Sci* 53:261–266
- Tanabe H, Ito Y, Terasaki H (2012) Choroid is thinner in inferior region of optic disks of normal eyes. *Retina* 32:134–139
- Unterhuber A, Považay B, Hermann B, Sattmann H, Chavez-Pirson A, Drexler W (2005) In vivo retinal optical coherence tomography at 1040 nm – enhanced penetration into the choroid. *Opt Express* 13:3252–3258
- Wei WB, Xu L, Jonas JB, Shao L, Du KF, Wang S, Chen CX, Wang YX, Zhou JQ, You QS (2013) Subfoveal choroidal thickness: the Beijing Eye Study. *Ophthalmology* 120:175–180
- Yamashita T, Shirasawa M, Arimura N, Terasaki H, Sakamoto T (2012) Repeatability and reproducibility of subfoveal choroidal thickness in normal eyes of Japanese using different SD-OCT devices. *Invest Ophthalmol Vis Sci* 53:1102–1107
- Yoneya STMM (1987) Angioarchitecture of the human choroid. *Arch Ophthalmol* 105:681–687
- Zhang H (1994) Scanning electron-microscopic study of corrosion casts on retinal and choroidal angioarchitecture in man and animals. *Prog Retin Eye Res* 13:243–270